RSC Advances

PAPER

View Article Online
View Journal | View Issue

Cite this: *RSC Adv.*, 2024, **14**, 1114

Myco-synthesis of multi-twinned silver nanoparticles as potential antibacterial and antimalarial agents†

Suresh kumar,[a] Megha Pant,[a] Cherish Prashar,[bc] Kailash C. Pandey,[bc] Subhasish Roy,[d] Veena Pande[a] and Anirban Dandapat *[e]

Received 13th November 2023
Accepted 28th November 2023

DOI: 10.1039/d3ra07752g

rsc.li/rsc-advances

In recent days, biogenic and green approaches for synthesizing nanostructures have gained much attention in biological and biomedical applications. Endophytic fungi have been recognized to produce several important biomolecules for use in various fields. The present work describes the use of endophytic fungi isolated from *Berberis aristata* for the synthesis of multi-twinned silver nanoparticles (MT-AgNPs) and their successful applications in antimicrobial and antimalarial studies. TEM images reveal the formation of multi-twined structures in the synthesized silver nanoparticles. The synthesized MT-AgNPs have shown excellent antibacterial activities against five opportunistic bacteria, *viz. Bacillus subtilis* (MTCC 441), *Pseudomonas aeruginosa* (MTCC 424), *Escherichia coli* (MTCC 443), *Klebsiella pneumonia* (MTCC 3384), and *Aeromonas salmonicida* (MTCC 1522). The synthesized MT-AgNPs also exhibit interesting antimalarial activities against *Plasmodium falciparum* parasites (3D7 strain) by displaying 100% inhibition at a concentration of 1 μg mL^{-1} against the malaria parasite *P. falciparum* 3D7. Overall, the results describe a green method for the production of twinned-structured nanoparticles and their potential to be applied in the biomedical, pharmaceutical, food preservation, and packaging industries.

1. Introduction

Mycosynthesis of nanomaterials has attracted a great deal of interest over conventional physicochemical methods because of their economical, non-toxic nature, and productivity of biocompatible nanoparticles, which are highly desirable for all different applications, especially biological ones.[1–3] Among different nanomaterials, silver nanoparticles are notable for their broad-spectrum biological applications.[4–6] However, their activities strongly depend on controlling the exterior surface structure of the nanoparticles. In recent years, it has been established that the multiple-twinned structure of the nanoparticles could increase the degree of exposure of the active Ag atoms and allow full exploitation of their activities.[7–9] Multi-twinned Ag nanoparticles (MT-AgNPs) thus showed enhanced activities in comparison to normal spherical particles. Most of the previous reports of biologically synthesized metal nanoparticles produced normal spherical particles.[10–13] Very recently, we reported endophyte-induced cuboid-shaped silver nanoparticles.[14] Endophytes provide a wide variety of bioactive metabolites (*e.g.*, alkaloids, flavonoids, phenols, steroids, *etc.*) with distinctive properties that can be exploited in improving synthesis methods for applications.[15–17] Therefore, it demands extensive research on the myco-synthesis utilizing various endophytes and their applications in different biological fields. In the present study, *Berberis aristata*, an important native medicinal plant in India, was investigated for the isolation of the endophytic fungus and then utilized in synthesizing MT-AgNPs, followed by their antimalarial and antibacterial activities.

Malaria is one of the most threatening human diseases caused by insect bites, which are able to cause infection by introducing different species of Plasmodium into the host.[18] These blood parasites have approximately 156 named species of plasmodium, which are harmful to various species of vertebrates. Out of which, four species are considered true parasites of humans, as they utilize humans as a natural intermediate host: *P. falciparum*, *P. vivax*, *P. ovale*, and *P. malariae*. Among them, *P. falciparum* is considered a dangerous and lethal parasite infecting humans because this species has particular virulence, which derives from its ability to subvert the physiology of its host during the blood stages of its development.[19,20] However, despite the current drugs accessible for the cure of

[a]*Department of Biotechnology, Kumaun University, Sir J. C. Bose Technical Campus, Bhimtal, Nainital, Uttarakhand 263136, India*
[b]*ICMR-National Institute of Malaria Research (NIMR), Delhi 110077, New Delhi, India*
[c]*Academic of Scientific and Innovative Research (AcSIR), Ghaziabad, India*
[d]*Department of Chemistry, Birla Institute of Technology and Science, K K Birla Goa Campus, Pilani, Goa 403726, India*
[e]*University School of Automation and Robotics, Guru Gobind Singh Indraprastha University, East Delhi Campus, SurajmalVihar, Delhi 110092, India. E-mail: dranirbandandapat@kunainital.ac.in*

† Electronic supplementary information (ESI) available. See DOI: https://doi.org/10.1039/d3ra07752g

this disease, it seems that, despite the effectiveness of available therapeutics, the main threat connected to this blood parasite is the emergence of drug resistance.[21,22]

The global augmentation of bacterial resistance to conventional antibiotics is another severe concern in the medical field. The high incidence of multidrug-resistant bacteria among bacteria-based infections decreases the efficiency of current treatments and causes thousands of deaths. The surplus and misuse of antibiotics in different veterinary and human-related diseases are common things, but the negative consequence of this is to create antibiotic resistance among the bacterial species. The long-term persistence of these drugs in the environment becomes the main reason for the development of antibiotic resistance genes in microbial flora.[23,24] Fortunately, the use of bactericidal nanoparticles could solve the threat, as most of the drug resistance mechanisms are extraneous to nanoparticles. In the literature, nanoparticle-induced antimicrobial studies suggest their direct contact with the bacterial cell wall without the need for penetrating the cell wall.[25–27] This raises the hope that the nanoparticles will not only be less susceptible to promoting resistance against bacteria but also in other biomedical applications. In this context, silver nanoparticles with suitable structure and functionalities have been applied in the biomedical and other health-related areas of modern world. This has motivated us to explore the mycosynthesis of multi-twinned silver nanoparticles and their applications in antibacterial and antimalarial activities. Herein, we describe the isolation of endophytic fungi from *Berberis aristata* and their utilization in the formation of silver nanoparticles. Finally, the synthesized MT-AgNPs have shown enhanced antimalarial and bactericidal activities. Biosynthesized nanoparticles can play a significant role in a future solution against malaria drug resistance by introducing the new drugs at the nanoscale or building active nanoparticles to be used against the blood parasite.

2. Experimental

2.1 Isolation of endophytc fungi

The endophytic fungi were isolated using a given method by Strobel *et al.*, with minor modifications.[28] The fresh leaves of *Berberis aristata* were collected in a sterilized, airtight specimen bag, and within 24 hours they were gently rinsed with running tap water to remove the adhering particles. The leaves were sectioned into 2 mm blocks and again surface sterilized with 70% ethanol for one minute, then soaked in sodium hypochlorite solution (4%) for three minutes, and rinsed with 70% alcohol again for one minute. The cutting sections were finally rinsed with sterilized distilled water at least four times and dried on sterilized filter paper. The final water was taken as a control to check the complete sterilization process. These sections of leaves were then inoculated onto Potato Dextrose Media and incubated at 28 °C for fungal hyphae growth. The periodic checking was done for fungal growth. There is a mixture of fungal hyphae that starts to grow after a few days; now subculture them again onto PDA plates for the isolation of pure colonies.

2.2 Phenotypic and genotypic identification of endophytic fungi

The morphological features of the fungus were identified with the help of lactophenol blue dye and the external structure of the fungus. The DNA of the fungus was isolated with the help of the CTAB method. The purified DNA is used as the template for PCR to amplify a segment of about 600 bp of the ITS gene sequence. Universal primers (ITS1 5′-TCCGTAGGTGAACCTGCGG-3′ and ITS4 5′-TCCTCCGCTTATTGATATGC-3′) were used. A single PCR sample containing 1 μL of DNA was amplified in a 20 μL reaction mixture containing 10X BUFFER, each deoxynucleoside triphosphate at 0.2 mM, each primer at 0.5 μM, and 2U of Taq polymerase (R001C TaKaRaTaqTM) per mL. PCRs were subjected to initial denaturation for 3 min at 95 °C and then 32 cycles of denaturation for 30 s at 95 °C, annealing at 50 °C for 30 s and extension cycle at 72 °C for 10 min. Twenty microliters of the reaction mixtures were analyzed on 1.5% agarose/Tris-Cl-sodium acetate-EDTA in the presence of 0.5 μg of ethidium bromide per mL and photographed under UV illumination. The positive amplicons were purified using the Favorprep™ GEL/PCR Purification Kit (Cat No. FAGCK001). The purified product was sequenced with Sanger's method of DNA sequencing in both directions. The MEGA X (Molecular Evolution Genetics Analysis) software was used to construct the phylogenetic tree. The homologous sequences related to the isolate were selected, and multiple sequence alignments were carried out using the ClustalW program in MEGA X software. The neighbor joining algorithm with 1000 bootstrap replications was used for the construction of the phylogenetic tree. The fungal identity was retrieved from NCBI GenBank.

2.3 Preparation of the extract and synthesis OF Ag NPs

Potato Dextrose Broth (PDB) 500 mL was used to prepare the extract of endophytic fungi. An agar disc containing endophytic fungi was incubated at 28 °C on an incubator shaker at 180 rpm for 21 days. Fungal biomass was filtered after the mentioned incubation period using muslin cloth and mixed with an equal volume of butanol. The two layers have been formed: the upper layer is the organic layer containing secondary metabolites, and the lower layer contains the remaining media. After air drying the organic layer, the remaining aqueous solution of 1 mM $AgNO_3$ was prepared by using 21.2 mg of $AgNO_3$ powder in 125 mL of Milli-Q water in a brown bottle and incubating at room temperature. A 90 millilitre aqueous solution of 1 mM silver nitrate was reduced using 10 mL of DMSO containing secondary metabolites of endophytic fungi at room temperature for 12 hours, resulting in a brown-reddish solution indicating the formation of AgNPs.

2.4 Characterization techniques and instrumentations

The extracellular synthesis of MW-AgNPs by endophytic fungi extract was initially detected by visual inspection for color changes of the cultured flask solutions from transparent to brown, then reddish brown, and then the synthesis was

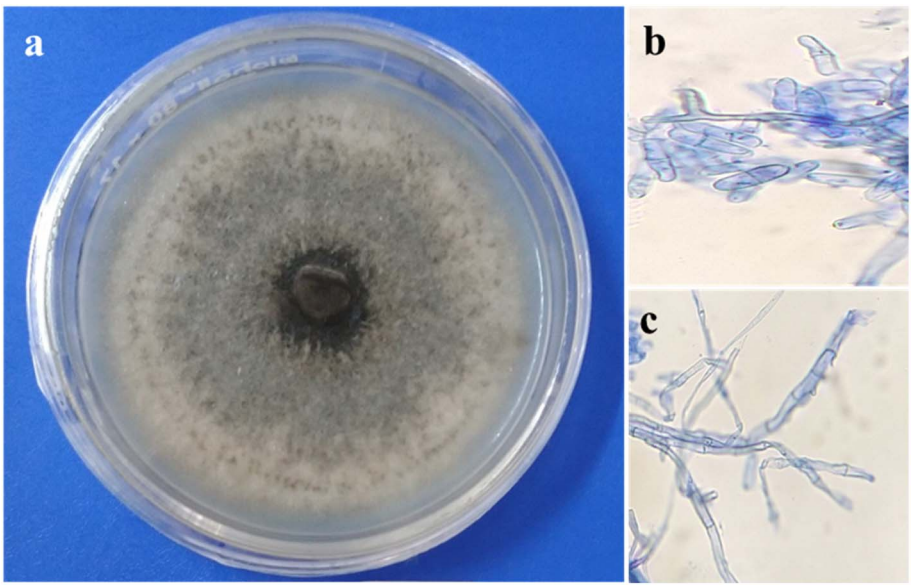

Fig. 1 Reproductive structures of the endophytic fungal isolates as seen under a compound microscope: (a) macroscopic aspects of *Colletotrichum gloeosporioides* after eight days on PDA medium; spores (b) and septate hyphae (c) of *Colletotrichum gloeosporioides* stained with cotton blue.

characterized through a UV-Vis spectrophotometer (Thermo Scientific Evolution 260 B10) and Fourier Transform Infrared spectroscopy (FTIR; PerkinElmer Spectrum 2). In addition, the FTIR spectrum data confirmed the presence of specific functional groups such as proteins, which do play an important role as a capping and stabilizing agent in the biosynthesis of AgNPs.[29] Secondary metabolites from endophytic fungi could play an instrumental role as an excellent candidate for nanoparticle biosynthesis. The crystalline nature of the synthesized AgNPs was confirmed by X-ray crystallography (Bruker D8

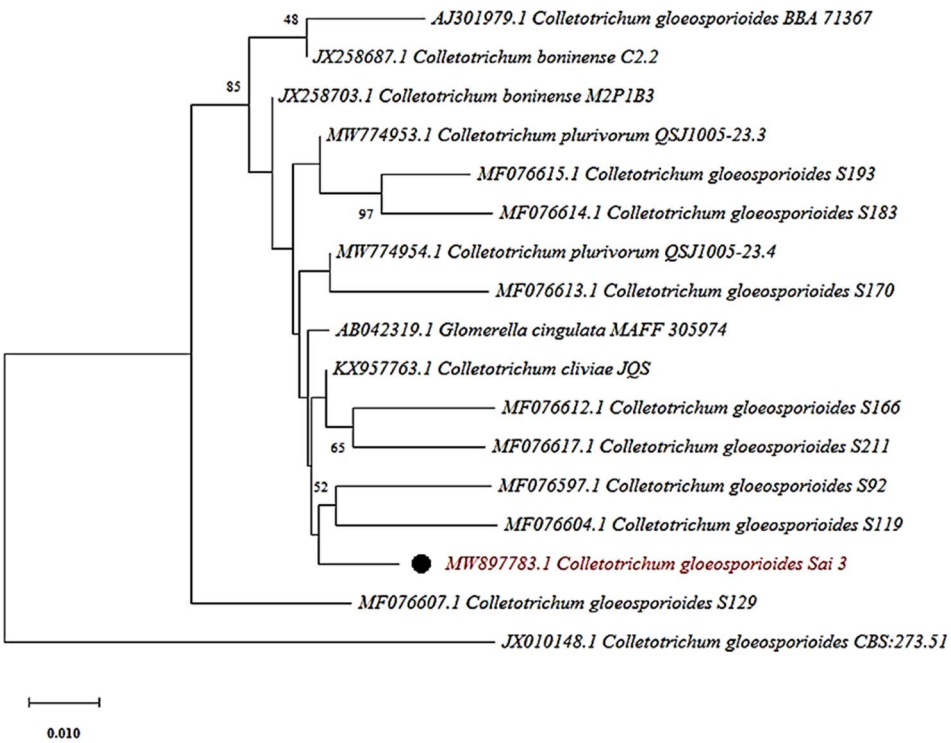

Fig. 2 Phylogenetic tree obtained from the neighbour-joining algorithm demonstrating the close association of the isolated strain *Colletotrichum gloeosporioides* (Sai 3) with other *Colletotrichum gloeosporioides* strains, and bootstrap values are given at the node.

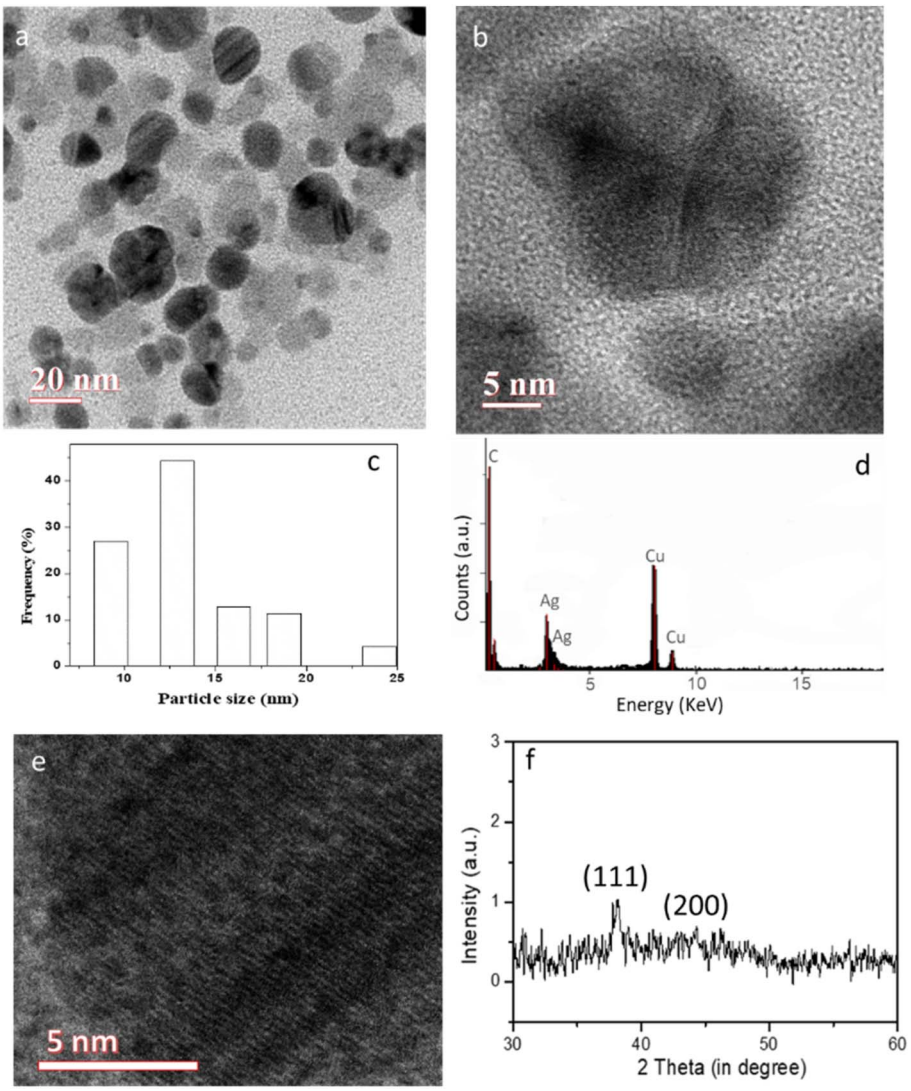

Fig. 3 (a–e) TEM images of the synthesized multi-twinned silver nanoparticles: (a) low and (b) high magnification TEM image, (c) histogram and (d) EDX analysis of the particles and corresponding (f) XRD pattern.

Advance). HRTEM images of the nanoparticles were taken with a Tecnai G2 20 S-TWIN [FEI] transmission electron microscope with an accelerating voltage of 200 kV.

2.5 Antibacterial susceptibility test

Antibacterial susceptibility tests were performed against opportunistic bacterial strains using the agar-well diffusion method. The five opportunistic bacterial strains used in the experiment were *Bacillus subtilis* (MTCC 441), *Pseudomonas aeruginosa* (MTCC 424), *Escherichia coli* (MTCC 443), *Klebsiella pneumonia* (MTCC 3384), and *Aeromonas salmonicida* (MTCC 1522). Firstly, the bacterial cultures were revived using an incubator at 37 °C at 200 rpm for 24 hours. The overnight bacterial broth was consistently distributed on nutrient agar with a cotton swap. Ampicillin disc was used as a standard antibiotic, and Silver salt was also added to the test as negative and positive controls, respectively. Previously, deionized water was used to dissolve the nanoparticles. The sterile tips were used to make wells in the agar plate and loaded with different volumes of 1 mg mL^{-1} concentration solution, such as 10 μL, 25 μL, 50 μL, and 100 μL samples, followed by incubation at 37 °C for 24 h. Afterward, the zone of inhibition was measured, and the assay was performed in triplicate.

2.6 Antimalarial activity

The *P. falciparum* parasite 3D7 strain was grown *in vitro* for an anti-malarial assay. The parasites were grown in fresh human erythrocytes (O+) and suspended in a mixture of 10.4 g L^{-1} RPMI 1640 (Gibco), 0.5% AlbuMAXI (Gibco), and 0.2% sodium bicarbonate (Sigma), and the pH was maintained at 7.2 in a gaseous environment of 5% CO_2 and 37 °C as described in previous studies. For the antimalarial assay, 3D7 cultures were synchronized using 5% sorbitol, and parasitemia was assessed. These 3D7 cultures were synchronized with 5% sorbitol for the

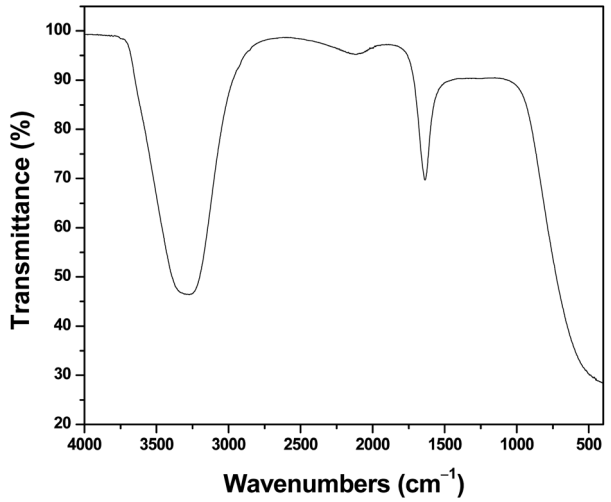

Fig. 4 FTIR spectra of the synthesized MT-AgNPs.

antimalarial assay, and parasitemia was assessed. *In vitro* synchronized ring-stage erythrocyte cultures of *P. falciparum* parasites were taken in a mixture of 5% haematocrit, and 0.5% parasitaemia in 96-well plates and treated with the biogenic AgNPs. The different concentrations of the nanomaterials were prepared, such as 50 μg mL^{-1} and 1 μg mL^{-1}, and incubated with the parasite culture in the treated wells at 37 °C and 5% CO_2 for 24 hours. Parasite growth and inhibition were assessed by fixing the thin blood smears in 100% methanol and staining them for 20–30 min in a 10% Giemsa stain solution. Chloroquine and DMSO served as the positive and negative controls for this assay at 37 °C in a 5% CO_2 environment in 96-well plates.

3. Results and discussion

Berberis aristata is an ethnomedicinal plant used to isolate various endophytic fungi for the development of silver nanoparticles. Healthy leaf tissues had been taken from the *Berberis aristata* plant. After a few days of incubation, the hyphae of the fungus started to appear. Several endophytic fungi were isolated, and among them, an endophyte (Sai-Three) isolated from the leaves shown in Fig. 1 has been selected for further morphological and molecular characterization based on its efficient activity against different pathogens. The direct microscopic study revealed the formation of septate hyphae. Fungal growth on potato dextrose agar media had non-aerial mycelia. The surface was a light pink coloured with a few blackish-brown dot on it. Conidia were acervuli and septate. The hyphae of the fungus were taken from potato dextrose agar plates for the isolation of DNA.

The isolated DNA of the fungus was used to amplify the internal transcribed spacer (ITS) region with the help of 18S rRNA universal primers ITS1 (forward) and ITS 4 (backward). The amplified DNA was then subjected to Sanger's sequencing and compared with standard sequences that have already been submitted to the NCBI Gene Bank. The comparative 18S rRNA gene analysis was carried out with the BLAST tool available at NCBI, with the help of this tool, the maximum homology of the isolated strain was matched with *Colletotrichum gloeosporioides*. The phylogenetic analyses showed the maximum closeness of the endophytic fungus with *Colletotrichum gloeosporioides* strains 119 and *Colletotrichum gloeosporioides Strains 92* (Fig. 2). These sequences were finally submitted to the NCBI Gene Bank database; the accession number for this fungus has been assigned as MW897783.1.

The bioactive molecules present in the fungal extracts are exploited for the synthesis of silver nanoparticles. A varying amount of extract was utilized to observe the role of concentrations of biomolecules on the reduction of silver ions and subsequent formation of silver nanoparticles. The reduction of silver ions into metallic silver nanoparticles was visualized by observing a color change from pale yellow to brownish red and a corresponding UV spectrum with a peak at ~450 nm (ESI; Fig. S1†).[30–32] HRTEM images show the formation of multi-twinned particles, as shown in Fig. 3a and b. HRTEM analysis revealed the generation of multi-twinned AgNPs with an average size of ~13 nm (Fig. 3c). EDX analysis shows the presence of silver and copper comes from TEM grid. A high-resolution image (Fig. 3c) reveals the fringe spacing of 0.24 nm, which can be indexed to Ag (111) crystal planes. The XRD pattern of the synthesized nanoparticles showed peaks at 38 and 44° 2θ, due to fcc Ag (111) and Ag (200) crystal planes.[33,34]

The FTIR spectrum (Fig. 4) was taken to analyse the functional groups present on the surface of the synthesized MT-AgNPs. The peak at ~3350 cm^{-1} can be assigned to O–H and N–H stretching vibrations. The peaks at 1639 cm^{-1} are assigned to the stretching vibration of the (NH) C=O group.[35,36] The peak at 1015 cm^{-1} can be attributed to the C–N stretching vibration

Table 1 The zones of inhibition were measured in the agar well diffusion plates during antimicrobial activity of MT-AgNPsagainst five selected pathogenic strains

	Agar-well diffusion (Zone of inhibition) mm			
Bacterial strain	10 μg mL^{-1}	25 μg mL^{-1}	50 μg mL^{-1}	100 μg mL^{-1}
Aeromonas salmonicida	10 ± 0.5 mm	11 ± 0.5 mm	12 ± 0.1 mm	14 ± 1 mm
Escherichia coli	No zone of inhibition	11 ± 0.5 mm	12 ± 0.1 mm	13 ± 1 mm
Bacillus subtilis	No zone of inhibition	10 ± 0.5 mm	11 ± 0.5 mm	12 ± 1 mm
Klebsiella pneumoniae	No zone of inhibition	No zone of inhibition	12 ± 0.7 mm	14 ± 0.2 mm
Pseudomonas aeruginosa	No zone of inhibition	10 ± 0.5 mm	11 ± 0.5 mm	12 ± 1 mm

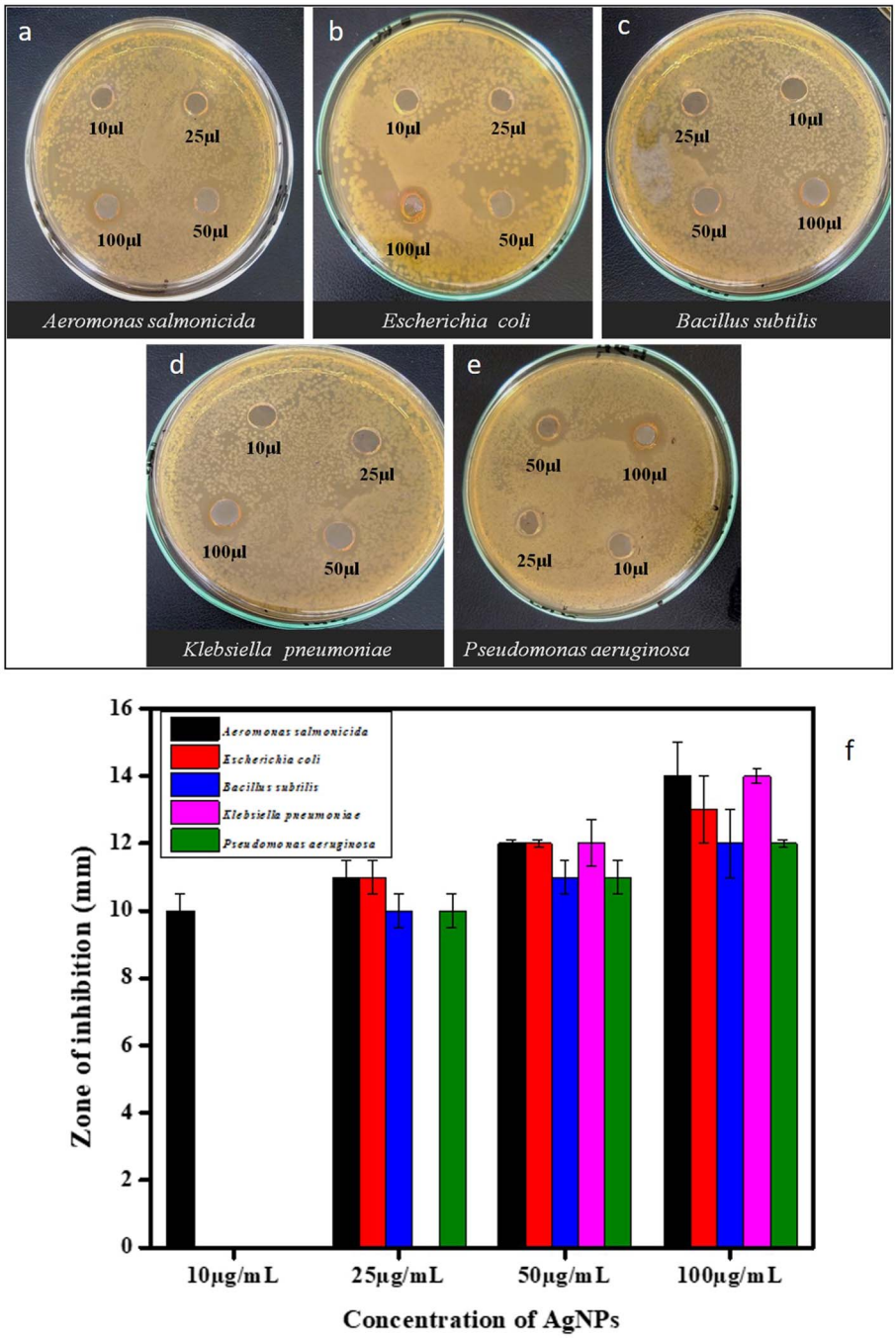

Fig. 5 Antibacterial activities of the synthesized MT-AgNPs: different doses (10–100 µg mL^{-1}) of MT-AgNPs against (a) *Aeromonas salmonicida*, (b) *Escherichia coli*, (c) *Bacillus subtilis*, (d) *Klebsiella pneumonia* and (e) *Pseudomonas aeruginosa* as mentioned in the figure. (f) Plot of calculated zone of inhibition *vs.* concentration of the MT-AgNPs.

mode. The presence of amines and amide groups in the endophytic fungus extracts imparts excellent capping and stabilizing properties to the silver nanoparticles for various biological applications.[37,38]

The antimicrobial efficacy of the synthesized MT-AgNPs was then studied against the five selected opportunistic bacterial species, *viz.*, *Bacillus subtilis* (MTCC 441), *Pseudomonas aeruginosa* (MTCC 424), *Escherichia coli* (MTCC 443), *Klebsiella pneumonia* (MTCC 3384), and *Aeromonas salmonicida* (MTCC 1522). Various concentrations (10–100 µg mL^{-1}) of biogenic MT-AgNPs were used, as indicated in Fig. 4, to check their activity against the selected bacteria. The synthesized MT-AgNPs showed excellent inhibitory activity against both Gram-positive and Gram-negative bacteria. Antimicrobial activities (Fig. 5) of the MT-AgNPs were checked by measuring the zone of inhibition against all the strains and found to vary from ~10–

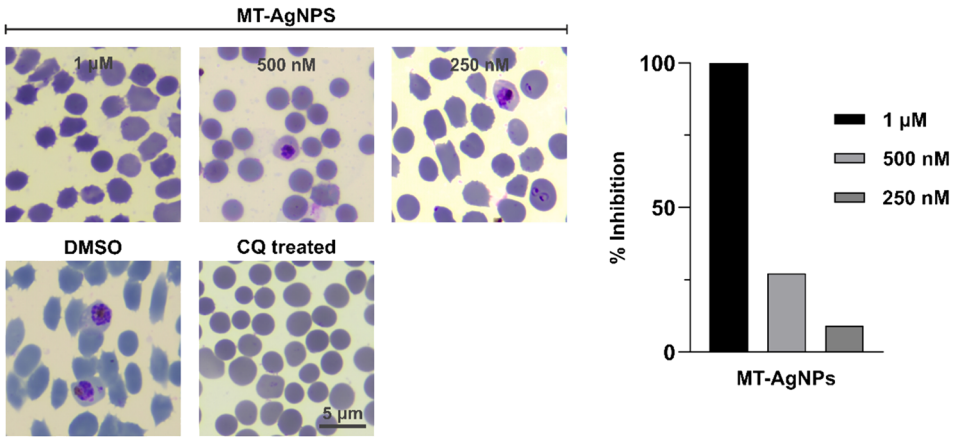

Fig. 6 Antimalarial activity of MT-AgNPs. Microscope slide images depict the inhibition of *Plasmodium* by the MT-AgNPs. At low concentrations of 250 nM and 500 nM, parasite is sick and deformed whereas at 1 μM concentration, parasite was completely inhibited. Negative control as DMSO shows the normal growth of parasites; positive control as Chloroquine displayed inhibition of the parasites. The graph represents the percent inhibition of the compound against *Plasmodium* according to different concentrations (1 μM, 500 nM, 250 nM).

15 mm with varying concentrations, as indicated in Table 1. A comparative analysis of the antimicrobial activities of the synthesized NPs (Table S1; ESI†) exhibits excellent activities of the synthesized MT-AgNPs.

There are several proposed mechanisms of action that have been considered behind the antibacterial activity, but these mechanisms are still not clearly understood. Previous literature data have shown a shred of evidence that the Ag^+ ions from these biogenic nanoparticles have a great potential of antibacterial activity.[39] These Ag^+ ions attack intracellularly with the peptidoglycan layer of the bacteria and may be the reason for inhibiting bacterial growth in three ways: firstly, they may be responsible for generating cellular oxidative stress at an extreme level and causing the generation of reactive oxygen species (ROS). Secondly, these biogenic Ag^+ ions have a good binding affinity for sulfur- and nitrogen-containing groups, and due to that, they are responsible for the distortion of the native protein structure by binding with thiols, a sulfhydryl group, a sulfanyl group, and amino groups of the protein. By attaching to these entities, may cause ROS induction, which directly impacts the respiratory enzymes and alters the Electron Transport Chain (ETC), which finally leads to the death of the cell. The third is to interrupt the DNA replication and translation mechanisms by disrupting the ribosome assembly, which finally stops the protein machinery, resulting in the cell's death.[40]

The antimalarial activities were assessed using the synthesized biogenic MT-AgNPs. The synthesized MT-AgNPs were screened for *in vitro* activity against the 3D7 strain of *P. falciparum*, and Chloroquine (CQ) was used as a control in the antimalarial assay, as shown in Fig. 6. Varying concentrations of MT-AgNPs (250 ng mL^{-1}, 500 ng mL^{-1}, and 1 μg mL^{-1}) were performed, and dose-dependent activity is depicted in Fig. 6. The data shows that an extremely low concentration (250 nM) of MT-AgNPs was also effective in showing antiplasmodial potential against *P. falciparum*. Moreover, 1 μg mL^{-1} could completely inhibit the growth of *P. falciparum*. It is believed that higher degrees of exposure of the active Ag atoms in the multi-twinning structures of MT-AgNPs are responsible for higher antibacterial and antiplasmodial activities.

4. Conclusions

This work reports a biogenic and economically viable approach for the synthesis of multi-twinned silver nanoparticles with efficient antibacterial and antimalarial activities. *Berberis aristata*, an ethnomedicinal plant, has been used to isolate various endophytic fungi, and among them, *Colletotrichum gloeosporioides* was successfully utilized in synthesizing multi-twinned silver nanoparticles. The synthesized MT-AgNPs have shown broad-spectrum antimicrobial activities against all the selected opportunistic bacterial species. Moreover, MT-AgNPs have also shown extremely high anti-malarial activities against the *Plasmodium falciparum* 3D7 strain. Therefore, the present approach not only provides a new synthetic method for multi-twinned nanoparticles but also opens up their wide biomedical applications.

Conflicts of interest

There are no conflicts to declare.

Acknowledgements

The authors would like to express deep gratitude for the support of DST, Govt. of India for financial assistance through the INSPIRE Faculty Award (IFA16-MS81).

References

1 Z. Pei, H. Leiand and L. Cheng, Bioactive inorganic nanomaterials for cancer theranostics, *Chem. Soc. Rev.*, 2023, **52**, 2031–2081.
2 J. Jeevanandam, S. F. Kiew, S. Boakye-Ansah, S. Y. Lau, A. Barhoum, M. K. Danquah and J. Rodrigues, Green

approaches for the synthesis of metal and metal oxide nanoparticles using microbial and plant extracts, *Nanoscale*, 2022, **14**(7), 2534–2571.

3 X. Yu, Z. Wang and Z. S. G. Wei, Design, fabrication, and biomedical applications of bioinspired peptide–inorganic nanomaterial hybrids, *J. Mater. Chem. B*, 2017, **5**(6), 1130–1142.

4 S. K. Balu, V. Sampath, S. Andra, S. Alagar and S. M. Vidyavathy, Fabrication of carbon and silver nanomaterials incorporated hydroxyapatite nanocomposites: Enhanced biological and mechanical performances for biomedical applications, *Mater. Sci. Eng. C*, 2021, **128**, 112296.

5 M. Shah, S. Nawaz, H. Jan, N. Uddin, A. Ali, S. Anjum, N. Giglioli-Guivarc'h, C. Hano and B. H. Abbasi, Synthesis of bio-mediated silver nanoparticles from Silybummarianum and their biological and clinical activities, *Mater. Sci. Eng. C*, 2020, **112**, 110889.

6 R. K. Gupta, V. Kumar, R. K. Gundampati, M. Malviya, S. H. Hasanand and M. V. Jagannadham, Biosynthesis of silver nanoparticles from the novel strain of Streptomyces Sp. BHUMBU-80 with highly efficient electroanalytical detection of hydrogen peroxide and antibacterial activity, *J. Environ. Chem. Eng.*, 2017, **5**(6), 5624–5635.

7 L. Yang, F. Meng, X. Qu, L. Xia, F. Huang, S. Qin, M. Zhang, F. Xu, L. Sun and H. Liu, Multiple-twinned silver nanoparticles supported on mesoporous graphene with enhanced antibacterial activity, *Carbon*, 2019, **155**, 397–402.

8 H. Yang, Y. Wang, X. Chen, X. Zhao, L. Gu, H. Huang, J. Yan, C. Xu, G. Li, J. Wu and J. A. Edwards, Plasmonic twinned silver nanoparticles with molecular precision, *Nat. Commun.*, 2016, **7**(1), 12809.

9 N. Murshid and V. Kitaev, Role of poly(vinylpyrrolidone)(PVP) and other sterically protecting polymers in selective stabilization of {111} and {100} facets in pentagonally twinned silver nanoparticles, *Chem. Commun.*, 2014, **50**(10), 1247–1249.

10 S. Li, Y. Shen, A. Xie, X. Yu, L. Qiu, L. Zhang and Q. Zhang, Green synthesis of silver nanoparticles using *Capsicum annuum* L. extract, *Green Chem.*, 2007, **9**(8), 852–858.

11 C. Krishnaraj, G. E. Jagan, S. Rajasekar, P. Selvakumar, T. P. Kalaichelvan and N. Mohan, Synthesis of silver nanoparticles using Acalyphaindica leaf extracts and its antibacterial activity against water borne pathogens, *Colloids Surf., B*, 2010, **76**(1), 50–56.

12 R. W. Rolim, T. M. Pelegrino, B. Lima Araújo de, S. L. Ferraz, N. F. Costa, S. J. Bernardes, T. Rodigues, M. Brocchi and B. A. Seabra, Green tea extract mediated biogenic synthesis of silver nanoparticles: Characterization, cytotoxicity evaluation and antibacterial activity, *Appl. Surf. Sci.*, 2019, **463**, 66–74.

13 A. G. Kahrilas, M. L. Wally, J. S. Fredrick, M. Hiskey, L. A. Prieto and E. J. Owens, Microwave-assisted green synthesis of silver nanoparticles using orange peel extract, *ACS Sustain. Chem. Eng.*, 2014, **2**(3), 367–376.

14 A. Kumar, S. Kumar, K. Kiran, S. Banerjee, V. Pande and A. Dandapat, Myco-nanotechnological approach to synthesize silver oxide nanocuboids using endophytic fungus isolated from Citrus pseudolimon plant, *Colloids Surf., B*, 2021, **206**, 111948.

15 W. H. Zhang, C. Y. Song and X. R. Tan, Biology and chemistry of endophytes, *Nat. Prod. Rep.*, 2006, **23**(5), 753–771.

16 A. G. Strobel, Endophytes as sources of bioactive products, *Microbes Infect.*, 2003, **5**(6), 535–544.

17 V. V. Kadam, P. J. Ettiyappan and M. R. Balakrishnan, Mechanistic insight into the endophytic fungus mediated synthesis of protein capped ZnO nanoparticles, *Mater. Sci. Eng. B*, 2019, **243**, 214–221.

18 B. Nadjm, B. Amos, G. Mtove, J. Ostermann, S. Chonya, H. Wangai and H. Reyburn, WHO guidelines for antimicrobial treatment in children admitted to hospital in an area of intense Plasmodium falciparum transmission: prospective study, *BMJ*, 2010, 340.

19 E. Avitabile, N. Senes, C. D'avino, I. Tsamesidis, A. Pinna, S. Medici and A. Pantaleo, The potential antimalarial efficacy of hemocompatible silver nanoparticles from Artemisia species against P. falciparum parasite, *PLoS One*, 2020, **15**(9), e0238532.

20 J. N. White, S. Pukrittayakamee, T. T. Hien, A. M. Faiz, A. O. Mokuolu and M. A. Dondorp, Erratum: Malaria, *Lancet*, 2014, **383**(9918), 723–735.

21 L. Cui, S. Mharakurwa, D. Ndiaye, K. P. Rathod and J. P. Rosenthal, Antimalarial drug resistance: literature review and activities and findings of the ICEMR network, *Am. J. Trop. Med. Hyg.*, 2015, **93**(3 Suppl), 57.

22 J. Achan, J. Mwesigwa, P. C. Edwin and U. D'alessandro, Malaria medicines to address drug resistance and support malaria elimination efforts, *Expert Rev. Clin. Pharmacol.*, 2018, **11**(1), 61–70.

23 K. K. Sodhi, M. Kumar, B. Balan, S. A. Dhaulaniya, P. Shree, N. Sharma and K. D. Singh, Perspectives on the antibiotic contamination, resistance, metabolomics, and systemic remediation, *SN Appl. Sci.*, 2021, **3**(2), 1–25.

24 O. C. Okoye, S. E. Okeke, C. K. Okoye, D. Echude, A. F. Andong, I. K. Chukwudozie and D. C. Ezeonyejiaku, Occurrence and fate of pharmaceuticals, personal care products (PPCPs) and pesticides in African water systems: A need for timely intervention, *Heliyon*, 2022, e09143.

25 M. Gallardo-Godoy, U. Eckhard, M. L. Delgado, J. Y. Puente Roo de, M. Nogues-Hoyos, J. F. Gil and A. R. Perez, Antibacterial approaches in tissue engineering using metal ions and nanoparticles: From mechanisms to applications, *Bioact. Mater.*, 2021, **6**(12), 4470–4490.

26 S. N. Bisht, H. A. Tripathi, M. Pant, K. S. Upadhyay, G. N. Sahoo, S. P. S. Mehta and A. Dandapat, A facile synthesis of palladium nanoparticles decorated bismuth oxybromide nanostructures with exceptional photo-antimicrobial activities, *Colloids Surf., B*, 2022, **217**, 112640.

27 D. Pancholi, S. N. Bisht, V. Pande and A. Dandapat, Development of novel BiOBr0. 75I0. 25 nanostructures with remarkably High dark phase bactericidal activities, *Colloids Surf., B*, 2021, **199**, 111558.

28 G. Strobel, X. Yang, J. Sears, R. Kramer, S. R. Sidhu and M. W. Hess, Taxol from Pestalotiopsismicrospora, an

endophytic fungus of Taxuswallachiana, *Microbiology*, 1996, **142**(2), 435–440.

29 M. Katib-Al, Y. Shahri-Al and A. Niemi-Al, Biosynthesis of silver nanoparticles by cyanobacterium Gloeocapsa, *Int. J. Enhanc. Res. Sci. Technol. Eng.*, 2015, **4**(9), 115–135.

30 E. M. Patrascu-Barbinta, C. Ungureanu, M. S. Iordache, R. I. Bunghez, N. Badea and I. Rau, Green silver nanobioarchitectures with amplified antioxidant and antimicrobial properties, *J. Mater. Chem. B*, 2014, **2**(21), 3221–3231.

31 C. T. Prathna, N. Chandrasekaran, M. A. Raichur and A. Mukherjee, Biomimetic synthesis of silver nanoparticles by Citrus limon (lemon) aqueous extract and theoretical prediction of particle size, *Colloids Surf., B*, 2011, **82**(1), 152–159.

32 K. S. Gogoi, P. Gopinath, A. Paul, A. Ramesh, S. S. Ghosh and A. Chattopadhyay, Green fluorescent protein-expressing Escherichia coli as a model system for investigating the antimicrobial activities of silver nanoparticles, *Langmuir*, 2006, **22**(22), 9322–9328.

33 V. Gopinath, D. MubarakAli, S. Priyadarshini, M. N. Priyadharsshini, N. Thajuddin and P. Velusamy, Biosynthesis of silver nanoparticles from Tribulusterrestris and its antimicrobial activity: a novel biological approach, *Colloids Surf., B*, 2012, **96**, 69–74.

34 A. Dandapat, K. T. Lee, Y. Zhang, K. S. Kwak, C. E. Cho and H. D. Kim, Attomolar level detection of Raman molecules with hierarchical silver nanostructures including tiny nanoparticles between nanosized gaps generated in silver petals, *ACS Appl. Mater. Interfaces*, 2015, **7**(27), 14793–14800.

35 P. Yu, J. J. McKinnon, R. C. Christensen and A. D. Christensen, Imaging molecular chemistry of Pioneer corn, *J. Agric. Food Chem.*, 2004, **52**(24), 7345–7352.

36 A. Kumar, S. Kumar, K. Kiran, S. Banerjee, V. Pande and A. Dandapat, Myco-nanotechnological approach to synthesize silver oxide nanocuboids using endophytic fungus isolated from Citrus pseudolimon plant, *Colloids Surf., B*, 2021, **206**, 111948.

37 R. B. Cruz, L. A. Baptista, S. Ntim, P. Manidurai, S. Espinoza, C. Ramanan, R. C. Huerto and M. Sulpizi, Role of pH in the synthesis and growth of gold nanoparticles using L-asparagine: a combined experimental and simulation study, *J. Phys.: Condens. Matter*, 2021, **33**(25), 254005.

38 M. Chen, Y. G. Feng, X. Wang, T. C. Li, J. Y. Zhang and D. J. Qian, Silver nanoparticles capped by oleylamine: formation, growth, and self-organization, *Langmuir*, 2007, **23**(10), 5296–5304.

39 A. S. Ahmad, S. S. Das, A. Khatoon, T. M. Ansari, M. Afzal, S. M. Hasnain and K. A. Nayak, Bactericidal activity of silver nanoparticles: A mechanistic review, *Mater. Sci. Energy Technol.*, 2020, **3**, 756–769.

40 A. Mishra, K. N. Kaushik, M. Sardar and D. Sahal, Evaluation of antiplasmodial activity of green synthesized silver nanoparticles, *Colloids Surf., B*, 2013, **111**, 713–718.